Supporting Information

Cerny et al. 10.1073/pnas.1009304107

SI Materials and Methods

Gene Cloning. Low- and moderate-stringency library screenings for *Msx, Dlx*, and *Gdf5/6/7* genes were performed as previously described (1). *Barx*, *Gdf5/6/7a*, and *Gdf5/6/7b* exons were PCR amplified from adult lamprey genomic DNA according to standard methods. All other genes were isolated using RACE. Briefly, lamprey total embryonic RNA was isolated from embryos during the early stages of pharyngogenesis, through the onset of chondrogenesis [Tahara (2) st. 23–28] using the RNAqueous kit (Ambion). 5′ and 3′ RACE libraries were then constructed and cDNA ends were amplified using the GeneRacer kit (Invitrogen). Exact-match partially overlapping 5′ and 3′ RACE primers were designed using the preassembly *Petromyzon marinus* genome. Primer sequences for all exons and RACE products are available upon request. Phylogenetic analyses were performed using the neighbor-joining and maximum likelihood methods (3, 4).

Embryo Collection and Staging. Embryos for in situ hybridization were obtained from adult spawning-phase sea lampreys (*Petromyzon marinus*) collected from Lake Huron, MI, and kept in chilled holding tanks as previously described (5). Embryos were staged according to the method of Tahara (2), fixed in MEMFA (Mops buffer, EGTA, $MgSO_4$, and formaldehyde), rinsed in Mops buffer, dehydrated into methanol, and stored at –20 °C. Key stages examined were st. 25 and st. 26.5 which correspond to 12–13 d and 15 d postfertilization, respectively.

In Situ Hybridization. In our experience, full-length *P. marinus* riboprobes, or riboprobes generated against untranslated regions of *P. marinus* transcripts, give higher background than short riboprobes against coding sequences. We believe that this is because lamprey noncoding sequences, especially 3′ UTRs, often have an excessive GC-repeat content, causing corresponding riboprobes to hybridize nonspecifically to off-targets. To mitigate this, we made short 300- to 500-bp riboprobes against coding regions and used a high-stringency hybridization protocol (6, 7). Key parameters of this protocol include posthybridization washes at 70 °C and the use of a low-salt, low-pH hybridization buffer (50% formamide; 1.3× SSC, pH 5.0; 5 mM EDTA, pH 8.0; 50 μg/mL tRNA; 0.2% Tween-20; 0.5% CHAPS; and 100 μg/mL heparin).

Histology and Sectioning. After in situ hybridization, embryos were postfixed in 4% paraformaldehyde/PBS (4 °C, overnight), rinsed in PBS, cryo-protected with 15% sucrose/PBS, embedded in 15% sucrose, 20% gelatin/PBS (37 °C, overnight), and 20% gelatin/PBS (37 °C overnight), frozen in liquid nitrogen, and mounted in OCT compound (Miles). Cryo-sections of 10 μm were collected on Super Frost Plus slides (Fisher Scientific), counterstained using Nuclear Fast Red (Vector Laboratories), and dehydrated and mounted in DPX (Fluka). To facilitate comparisons of DV expression, sections were level-matched to the fifth pharyngeal arch using the posterior limit of the endostyle as a reference point. The endostyle extends from the second arch to the fifth arch, but is not seen in transverse sections through the sixth arch. We thus chose pharyngeal arch sections that included the endostyle and were immediately followed by a pharyngeal arch section lacking the endostyle. The level of the fifth arch was further confirmed by measuring the diameter of the endostyle relative to the gut. At pharyngeal arch 5, the endostyle is characteristically small relative to the gut because of the posterior tapering of the endostyle, measuring approximately half of the height of the gut cavity. The extent of DV expression was judged at this level using the dorsal limit of the gut cavity and DV extent of the endostyle as landmarks.

1. Sauka-Spengler T, Meulemans D, Jones M, Bronner-Fraser M (2007) Ancient evolutionary origin of the neural crest gene regulatory network. *Dev Cell* 13:405–420.
2. Tahara Y (1988) Normal stages of development in the lamprey *Lampetra reissneri* (Dybowski). *Zoolog Sci* 5:109–118.
3. Saitou N, Nei M (1987) The neighbor-joining method: A new method for reconstructing phylogenetic trees. *Mol Biol Evol* 4:406–425.
4. Schmidt HA, Strimmer K, Vingron M, von Haeseler A (2002) TREE-PUZZLE: maximum likelihood phylogenetic analysis using quartets and parallel computing. *Bioinformatics* 18(3):502–504.
5. Nikitina N, Bronner-Fraser M, Sauka-Spengler T (2009) Microinjection of RNA and morpholino oligos into lamprey embryos. *Cold Spring Harb Protoc* 2009:pdb.prot5123.
6. Henrique D, et al. (1995) Expression of a Delta homologue in prospective neurons in the chick. *Nature* 375:787–790.
7. Meulemans D, Bronner-Fraser M (2002) Amphioxus and lamprey AP-2 genes: Implications for neural crest evolution and migration patterns. *Development* 129:4953–4962.

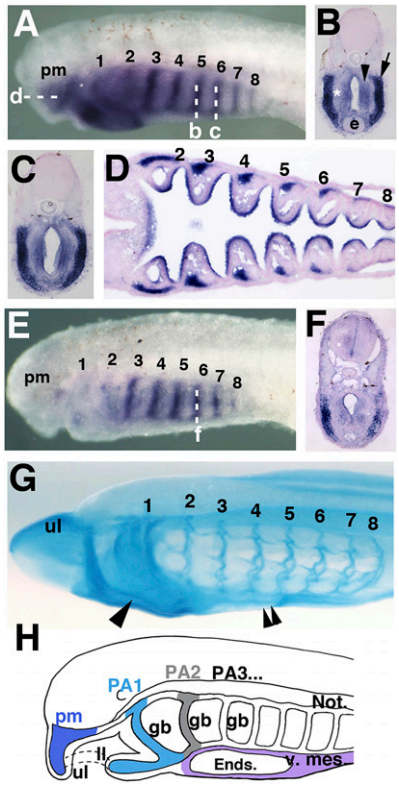

Fig. S1. Development of the head skeleton in *P. marinus.* (*A*) Postmigratory cranial neural crest cells at st. 26.5 visualized by in situ hybridization for a lamprey *Endothelin* receptor (*Ednr*). At this stage, all of the pharyngeal arches have formed, and CNCCs in the pharynx have condensed into bars but have not yet begun to form cartilage. *Ednrs* are robust, ubiquitous markers of postmigratory neural crest in diverse vertebrates. (*B*) Transverse section through *A* at the level of *b* showing *Ednr* expression in CNCC-derived mesenchyme throughout the DV extent of the fifth pharyngeal arch and in mesenchyme surrounding the endostyle (*e*). Note that whereas most of the pharyngeal CNCC (arrow) sits lateral to the pharyngeal mesoderm (asterisk), some CNCC are seen medial to the mesoderm (arrowhead), adjacent to the pharyngeal endoderm. (*C*) Transverse section through *A* at the level of *c,* the sixth pharyngeal arch. Note that the endostyle does not extend past the fifth pharyngeal arch and is not seen at this level of sectioning. (*D*) Horizontal section through *A* at the level of *d.* Strong *Ednr* expression is seen in CNCC lateral to the pharyngeal mesoderm. (*E*) *SoxE1* expression at st. 26.5. At this stage, *SoxE1* marks the forming "stack-of-coins" cartilage in the posterior arches, and does not label *Ednr*-expressing CNCC in the rest of the head. (*F*) Transverse section at the level of the sixth pharyngeal arch (*f* in *E*) showing *SoxE1* expression in the forming gill bars, but not in the ventral-most CNCC. (*G*) Alcian blue staining of a lamprey larva at st. 30+. At this stage, the cartilage bars have taken on their characteristic bent morphology and have begun projecting horizontal cross-bars. Alcian blue-positive mucocartilage is seen surrounding the endostyle (double arrowheads) and in the first arch (arrow) and upper lip (ul). (*H*) Schematic of a parasagittal section through the larval lamprey head at Tahara st. 26.5. Mesenchyme of the upper lip (ul) includes presumptive premandibular CNCC (pm). Lower lip (ll) and first gill bar (gb) are considered the dorsal and ventral aspects, respectively, of the first pharyngeal arch (PA1). The ventral mesenchyme (v. mes., purple) surrounds the endostyle (Ends.). The nascent pharyngeal skeleton abuts the notochord (Not.) dorsally.

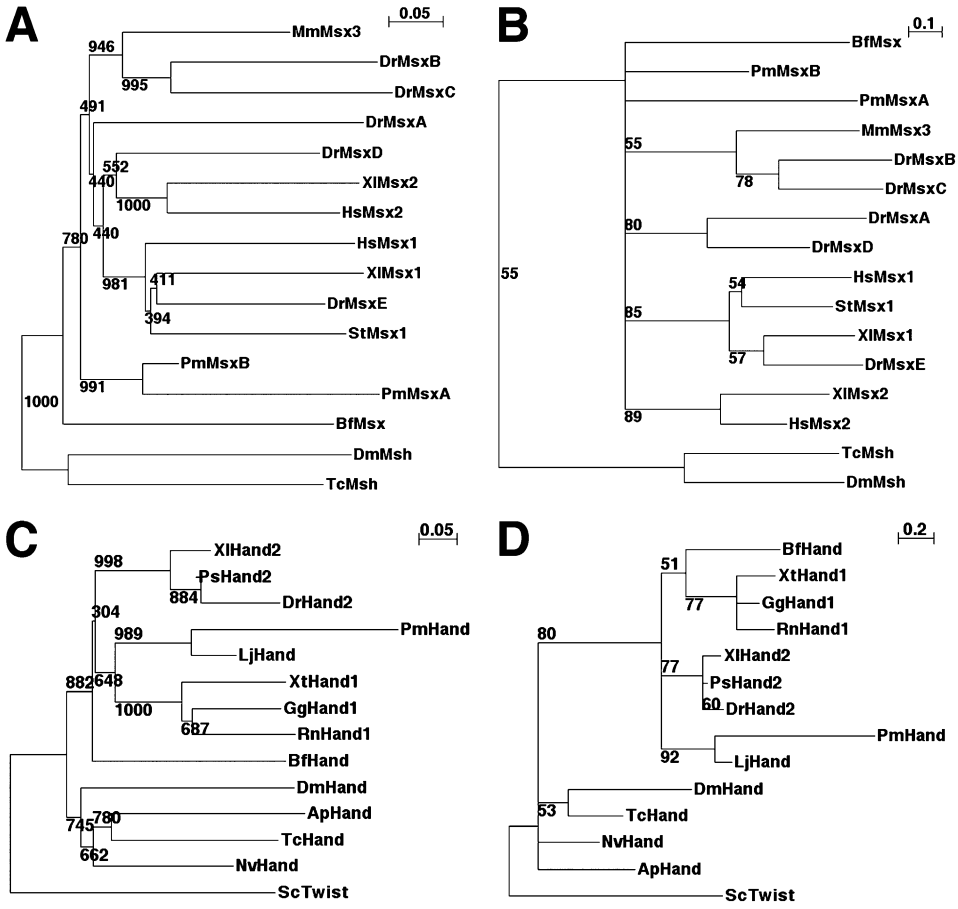

Fig. S2. Phylogenetic analyses of lamprey *Msx* and *Hand* genes. (*A* and *B*) Metazoan *Msx* gene phylogeny inferred using the neighbor-joining and maximum likelihood methods, respectively. Insect *Msh* genes serve as outgroup. (*C* and *D*) Metazoan *Hand* gene phylogeny inferred using the neighbor-joining and maximum likelihood methods, respectively. Distantly related bHLH transcription factor *Twist* from the shark, *Scyliorhinus canicula,* serves as the outgroup. Bootstrap values for neighbor-joining trees and quartet-puzzling reliability scores for maximum likelihood trees are shown at branch points. Distance units are shown in the upper right-hand corner of the trees. Gene names are prefixed by the initials of their respective species names. Species included in the analyses are *Brachiostoma floridae, Danio rerio, Gallus gallus, Nasonia vitripennis, Mus musculus, Homo sapiens, Petromyzon marinus, Drosophila melanogaster, Tribolium castaneum, Acyrthosiphon pisum, Lethenteron japonicum, Rattus norvegicus, Polyodon spathula, Scyliorhinus torazame, Scyliorhinus canicula, Xenopus laevis,* and *Xenopus tropicalis.*

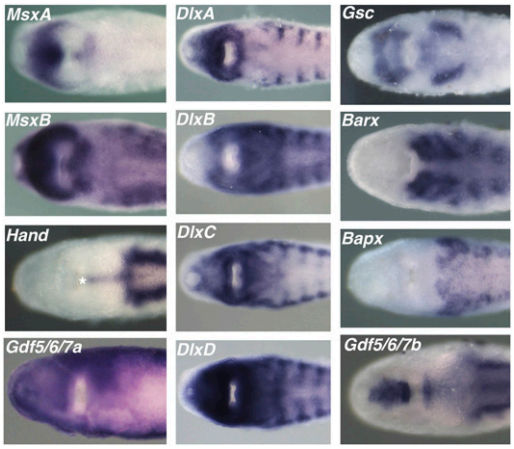

Fig. S3. Twelve genes involved in DV patterning of the gnathostome pharyngeal skeleton are differentially expressed around the larval lamprey mouth. Gnathostome-like combinatorial expression of these genes in the nascent oral skeleton of lamprey suggests that a high level of pharyngeal skeletal patterning was present in the first vertebrates.

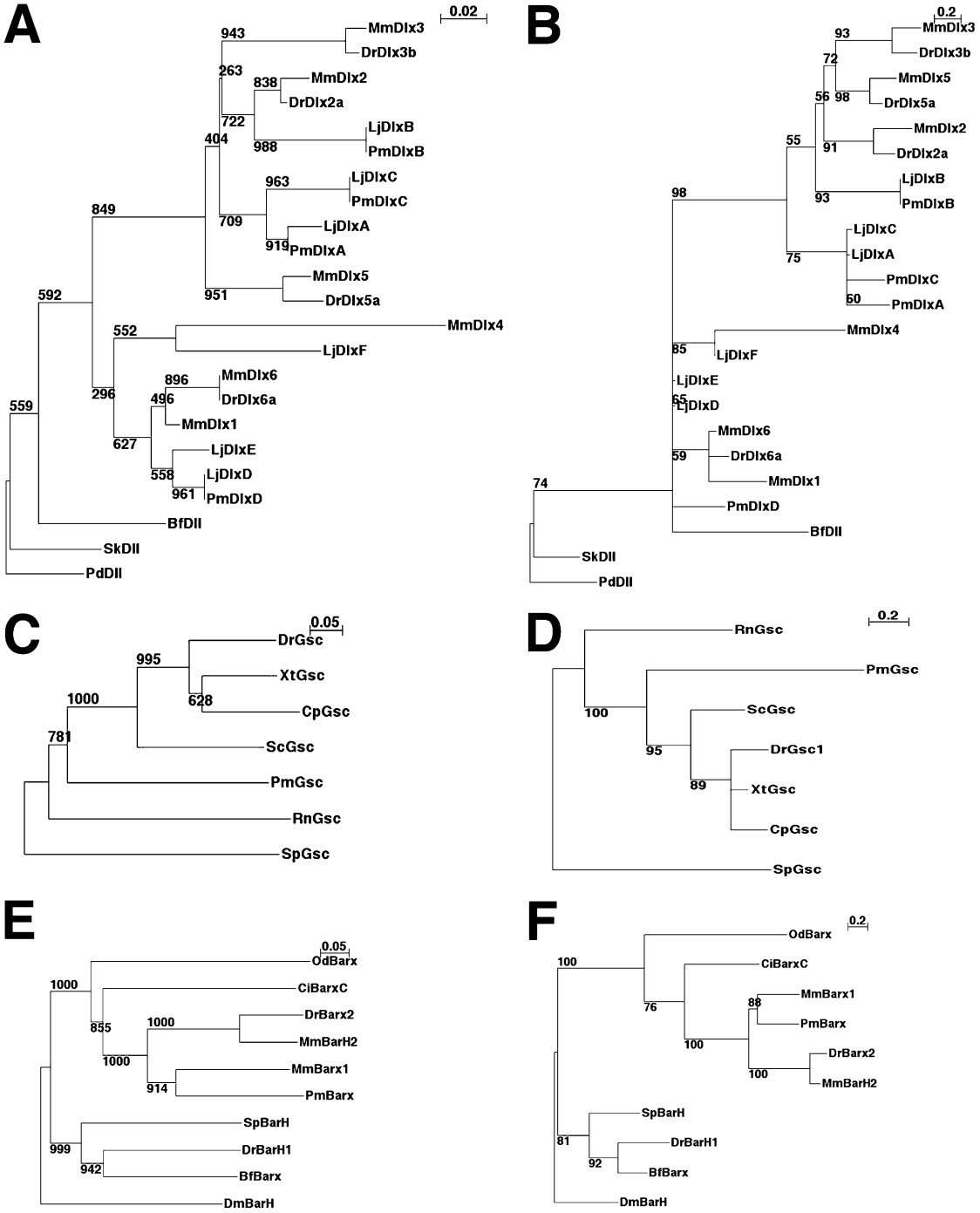

Fig. S4. Phylogenetic analyses of lamprey *Dlx, Gsc,* and *Barx* genes. (*A* and *B*) Metazoan *Dlx* gene phylogeny inferred using the neighbor-joining and maximum likelihood methods, respectively. *Platnereis dumerilii Dll* serves as the outgroup. (*C* and *D*) *Gsc* gene phylogeny inferred using the neighbor-joining and maximum likelihood methods, respectively. *S. purpuratus Gsc* serves as the outgroup. (*E* and *F*) *Barx* gene phylogeny inferred using the neighbor-joining and maximum likelihood methods, respectively. (*D*) *melanogaster BarH* serves as the outgroup. Bootstrap values for neighbor-joining trees and quartet-puzzling reliability scores for maximum likelihood trees are shown at branch points. Distance units are shown in the upper right-hand corner of the trees. Gene names are prefixed by the initials of their respective species names. Species included in the analyses are *Brachiostoma floridae, Ciona intestinalis, Strongylocentrotus purpuratus, Lethenteron japonicum, Saccoglossus kowalevskii, Platnereis dumerilii, Drosophila melanogaster, Rattus norvegicus, Danio rerio, Mus musculus, Oikopleura dioica, Petromyzon marinus, Cynops pyrrhogaster, Scyliorhinus canicula,* and *Xenopus tropicalis.*

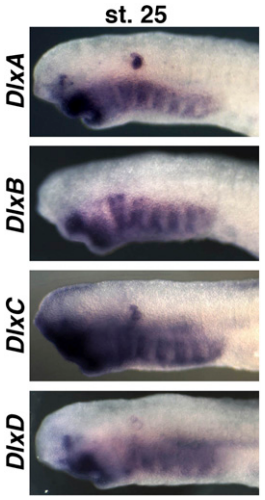

Fig. S5. Expression of lamprey *Dlx* genes at st. 25 (12–13 d at 18 °C). Differences in the DV extent of expression between the paralogs are less pronounced at this stage than at 26.5 (15–16 d at 18 °C). At this stage, postmigratory CNCC form mesenchymal sheets in the pharyngeal arches rather than the condensed bars seen at st. 26.5 (compare with Fig. S1).

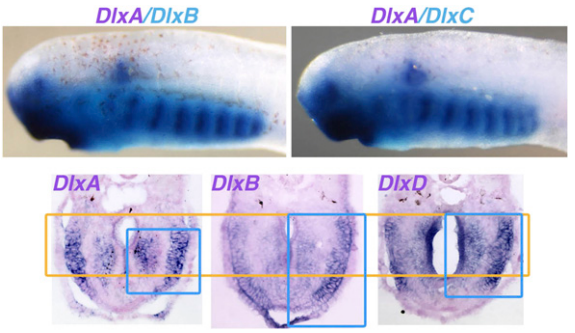

Fig. S6. Nested expression of *Dlx* genes at st. 26.5. Double in situ hybridizations for *DlxA* (purple) and *DlxB* (cyan), and for *DlxA* (purple) and *DlxC* (cyan). *DlxA* expression is nested within broader domains of *DlxB* and *DlxC* expression at this stage. Level- and stage-matched transverse sections showing DV extent of *DlxA*, *DlxB*, and *DlxD* expression in the sixth pharyngeal arch (blue boxes). Yellow box bounds the pharyngeal cavity and serves as a reference.

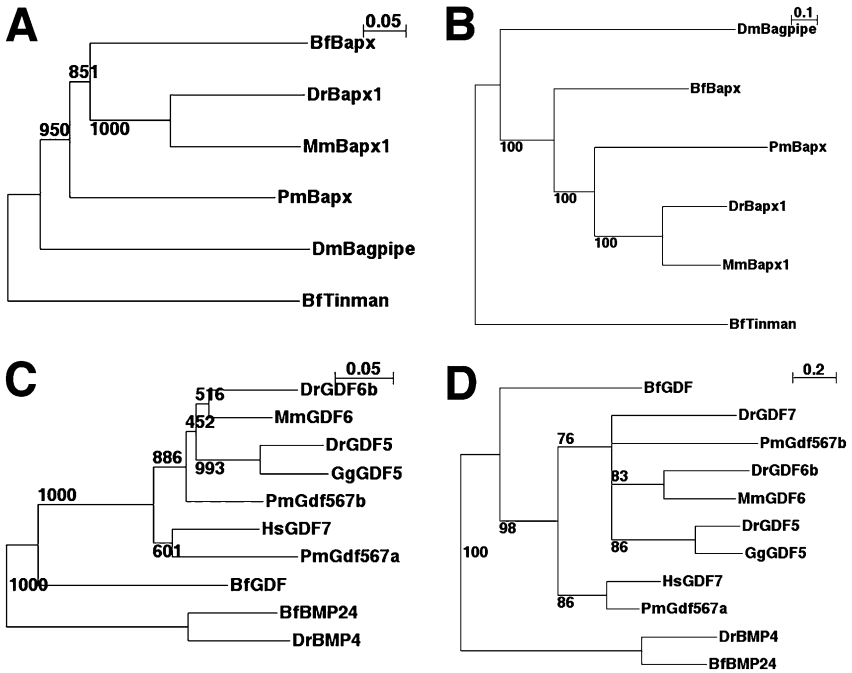

Fig. S7. Phylogenetic analyses of lamprey *Bapx* and *Gdf5/6/7*. (*A* and *B*) Metazoan *Bapx* gene phylogeny inferred using the neighbor-joining and maximum likelihood methods, respectively. The distantly related *Tinman* gene from *B. floridae* serves as the outgroup. (*C* and *D*) *GDF5/6/7* gene phylogeny inferred using the neighbor-joining and maximum likelihood methods, respectively. Related *TGF*β genes of the *BMP2/4* family from *D. rerio* and *B. floridae* serve as the outgroup. Bootstrap values for neighbor-joining trees and quartet-puzzling reliability scores for maximum likelihood trees are shown at branch points. Distance units are shown in the upper right-hand corner of the trees. Gene names are prefixed by the initials of their respective species names. Species included in the analyses are *Brachiostoma floridae, Drosophila melanogaster, Danio rerio, Mus musculus, Gallus gallus, Homo sapiens,* and *Petromyzon marinus.*

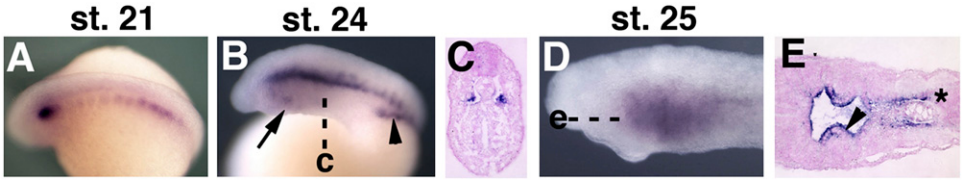

Fig. S8. Lamprey *Bapx* expression from st. 21–25. (*A*) Dorso-lateral view of st. 21 lamprey embryo showing *Bapx* expression in the somites in the trunk and paraxial mesoderm in the head. (*B*) Lateral view of the head at st. 24 showing *Bapx* expression in the paraxial mesoderm, pharyngeal ectoderm (arrow) and presumptive pronephros (arrowhead). (*C*) Transverse section at the level of *c* in *B* showing *Bapx* expression in the paraxial mesoderm at st. 24. (*D*) Expression of *Bapx* in the pharyngeal endoderm at st. 25. (*E*) Horizontal section at the level of *e* in *D* showing *Bapx* expression in pharyngeal endoderm (arrowhead) and paraxial mesoderm (asterisk).

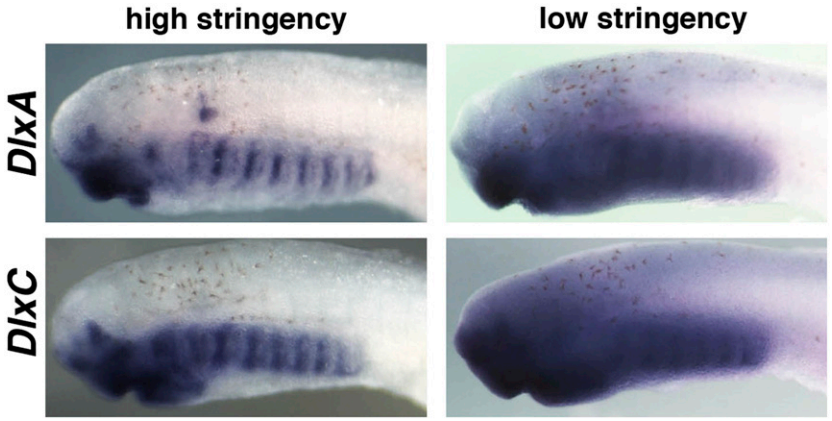

Fig. S9. Comparison of low-stringency and high-stringency in situ hybridization protocols. In situ hybridizations for *P. marinus DlxA* and *DlxC* were performed using either a low-stringency or high-stringency protocol. The low-stringency protocol was as described in Neidert et al. (1). The high-stringency protocol was as described in *Materials and Methods*. Key differences include washes at 70 °C and the use of a low-salt, low-pH hybridization buffer. In addition, Short, 500-bp riboprobes against *Dlx* coding sequences and were generated and GC-rich untranslated regions were avoided, as they tend to give high background signal in *P. marinus*.

1. Neidert AH, Virupannavar V, Hooker GW, Langeland JA (2001) Lamprey Dlx genes and early vertebrate evolution. *Proc Natl Acad Sci USA* 98:1665–1670.

Table S1. Numbers of larvae st. 25–28 analyzed by cryostat sectioning for each gene

Ventrally expressed	*Dlx* paralogs	First-arch patterning
MsxB: 10 larvae	*DlxA*: 7 larvae	*Gsc*: 9 larvae
dHand: 9 larvae	*DlxB*: 8 larvae	*Barx*: 8 larvae
	DlxC: 14 larvae	*Bapx*: 25 larvae
	DlxD: 7 larvae	*Gdf5/6/7b*: 7 larvae